Membrane Insertion and Antibody Recognition of a Glycosylphosphatidylinositol-Anchored Protein: An Optical Study†

J. J. Ramsden*

Department of Biophysical Chemistry, Biozentrum, 4056 Basel, Switzerland

P. Schneider

Institute of Biochemistry, Lausanne University, 1066 Epalinges, Switzerland

Received June 25, 1992; Revised Manuscript Received September 29, 1992

ABSTRACT: The kinetics of binding of a glycolipid-anchored protein (the promastigote surface protease, PSP) to planar lecithin bilayers is studied by an integrated optics technique, in which the bilayer membrane is supported on an optical wave guide and the phase velocities of guided light modes in the wave guide are measured. From these velocities, the optical parameters of the membrane and PSP layers deposited on the waveguide are determined, yielding in particular the mass of PSP bound to the membrane, which is followed in real time. From a comparison of the binding rates of PSP and PSP from which the lipid moiety has been removed, it is shown that the lipid moiety plays a key role in anchoring the protein to the membrane. Specific and nonspecific binding of antibodies to membrane-anchored PSP is also investigated. As little as a fifth of a monolayer of PSP is sufficient to suppress the appreciable nonspecific binding of antibodies to the membrane.

The promastigate stage of the protozoan parasite *Leishmania major* expresses at its surface an abundant metalloprotease (PSP)[1] of 63 kDa with an estimated radius of 2.7 nm, present at about 500 000 copies/cell (Bouvier et al., 1985). The protease is anchored to the membrane by means of a covalently attached glycosylphosphatidylinositol (GPI), which represents the unique site of interaction of the protease with the membrane (Bordier et al., 1986; Schneider et al., 1990).

Optical methods offer a convenient, noninvasive assay for measuring binding kinetics, and refractive index measurements are particularly convenient because they require no special radioactive, fluorescent, or other kind of labeling of the molecule under study. This means that not only is the risk of changing the properties of the molecule by labeling removed, but also the cumbersome workup stages required to complete the assay, which prevent the quantity of interest—in our case, the mass of protein bound—from being monitored continuously in real time, are eliminated.

The problem is then how to measure the refractive index of ultrathin layers such as membranes. It is known that the phase velocities of guided light modes propagating in optical waveguides are sensitive to the immediate environment of the waveguide (Tien, 1971). Hence, the refractive index and thickness of a lipid membrane or a protein layer deposited on a waveguide can be determined by measuring these velocities. From the refractive index and thickness of a protein layer, the deposited mass can be calculated (Ramsden, 1992). The precision of the measurements is extremely high, allowing surface mass density to be determined with an error of less than 1 ng/cm^2. Measurements can be carried out in real time, with a time resolution of a few seconds in the present apparatus, suitable for many biological binding reactions. The aim of this work was to exploit this precision to deepen our knowledge of the binding of lipid-anchored proteins to membranes, as well as the binding of antibodies to these proteins.

Several related techniques are currently being applied to investigate lipid monolayers, such as Brewster angle microscopy (Hönig & Möbius, 1991), surface plasmon microscopy (Schmitt et al., 1990), and phase-contrast microscopy (Takoshima et al., 1992). These techniques provide spatial resolution, although not at molecular level, for which atomic force microscopy is more suitable (Hoh & Hansma, 1992). The main advantage of the technique used in this paper is that it is applicable to *bilayers*; many protein adsorption and binding phenomena, especially those involving lipid-anchored proteins, require the use of a bilayer rather than a monolayer for the study of those aspects of lipid–protein interactions relevant to biology.

EXPERIMENTAL PROCEDURES

Background of the Method. If light of wavelength λ is directed with angle of incidence α onto a diffraction grating impressed into the surface of a planar waveguide (see Figure 1), the light will be coupled into the waveguide, provided that the following relation holds (Tiefenthaler & Lukosz, 1989):

$$N = n \sin \alpha + l\lambda/\Lambda \quad (1)$$

Here N is the effective refractive index[2] of the composite waveguide structure comprising glass support, waveguide, one or more thin films deposited on the waveguide, and buffer; n is the refractive index of the medium (air) surrounding the waveguide; l is the diffraction order; and Λ is the line spacing of the grating. N is highly sensitive to the immediate environment of the waveguide proper, because the electric field of the guided waves extends for some distance into the

† This work was supported in part by the Swiss National Science Foundation (Grant 32-28872.90).

* Author to whom correspondence should be addressed.

[1] Abbreviations: PSP, promastigote surface protease; H-PSP, hydrophilic PSP (i.e., lacking the lipid anchor); GPI, glycosylphosphatidylinositol; PBS, phosphate-buffered saline; PI-PLC, phosphatidylinositol-specific phospholipase C; POPC, 1-palmitoyl-2-oleoylphosphatidylcholine.

[2] N is defined as the ratio of the phase velocities of light in vacuum and in the waveguide.

0006-2960/93/0432-523$04.00/0 © 1993 American Chemical Society

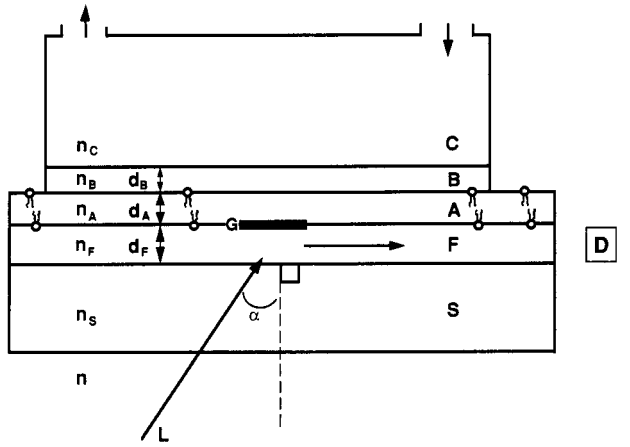

FIGURE 1: Schematic diagram of the experimental setup. S, glass support; F, wave-guiding film; A, lipid membrane; B, bound protein layer; C, cuvette filled with buffer solution; G, diffraction grating; L, incident light beam; D, detector (photodiode). n and d are, respectively, the refractive indices and thicknesses of the layers.

surrounding medium (Tien, 1971). The relationship between N and the unknown parameters n_A, d_A, n_B, and d_B, i.e., the refractive indices n and thicknesses d of the lipid membrane (subscript A) and protein thin film (subscript B), is provided by the mode equations for the guided waves (Spikhalskii, 1986; Tiefenthaler & Lukosz, 1989; Ramsden, 1992).

Materials and Methods. PSP was purified from promastigotes of *L. major* (strain LEM 513) by a temperature-induced phase separation in the detergent Triton X-114, followed by two steps of anion-exchange chromatography, as described by Bouvier et al. (1985, 1989). PSP was converted to its hydrophilic form (H-PSP) using *Trypanosoma brucei* glycosylphosphatidylinositol-specific phospholipase C as described previously (Bordier et al., 1986). The protein was then rechromatographed through the final anion-exchange step of the purification (Bouvier et al., 1989). Preimmune and immune rabbit sera directed against native PSP were as described by Bouvier et al. (1985) and were kindly provided by Dr. J. Bouvier (University of Lausanne, Epalinges, Switzerland). Sera were loaded at 0.5 mL/min onto a protein G–Sepharose column (10 × 1 cm, Pharmacia, Uppsala, Sweden), equilibrated in 10 mM NaH_2PO_4/Na_2HPO_4 at pH 7.2 plus 140 mM NaCl (PBS), and the column was washed with PBS. The IgGs were eluted at a flow rate of 6 mL/min with 0.1 M glycine hydrochloride at pH 2.7, immediately neutralized with 0.1 volume of 1 M Tris-HCl at pH 9.5, and dialyzed against PBS. The concentration was determined by measurement of the optical density at 280 nm (where an optical density of 1.4 corresponds to 1 mg/mL).

Rabbit polyclonal antibodies directed against a mitochondrial matrix protease were a kind gift from Philipp Scherer, Biozentrum, Basel, Switzerland.

Phosphatidylinositol-specific phospholipase C (PI-PLC) from *Bacillus thuringiensis*, a kind gift of Dr. M. G. Low (Columbia University, New York) was used at 1 unit/mL in PBS.

Planar optical wave guides incorporating a grating coupler with line density Λ^{-1} = 2400 mm^{-1} were obtained from ASI AG, Zürich, Switzerland (type 2400). The wave-guiding layer, with a thickness d_F of ca. 170 nm, is made from a mixture of SiO_2 and TiO_2 with a refractive index n_F of ca. 1.8 relative to air and is supported on a glass substrate. Before use, the waveguides were soaked overnight in PBS.

A 1 mM solution of 1-palmitoyl-2-oleoylphosphatidylcholine (POPC; Avanti Polar Lipids Inc., Alabaster, AL) was made up in 9:1 hexane/ethanol and spread on a laboratory-built Langmuir trough (area 150 cm^2) filled with PBS. After the lipids were compressed to a surface pressure of 32 mN/m, the first monolayer was deposited on the waveguide with the polar headgroups oriented next to its hydrophilic surface by slowly withdrawing the waveguide vertically out of the trough (Langmuir–Blodgett technique) while maintaining the surface pressure at 32 mN/m. The second monolayer was deposited by then rapidly lowering the waveguide horizontally onto and through the floating monolayer (Langmuir & Schaefer, 1937). The waveguide was then mounted with the grating facing upward in an integrated optics scanner (IOS-1, ASI AG, Zürich, Switzerland), and a small flow-through aluminum cuvette (volume = 0.07 cm^3) was sealed with an O-ring over the grating region. The waveguide therefore forms one wall (area = 0.785 cm^2) of the cuvette. The other surfaces of the cuvette exposed to the solution were electrochemically passivated, and any remaining protein binding sites were blocked by prior incubation with protein solution. The light beam from a He–Ne laser (λ = 632.82 nm, diameter = 0.8 mm) is directed against the grating from below. In order to measure the angle of incidence α, the table on which the waveguide is mounted is rotated while the intensity of the incoupled light is measured by photodiodes positioned at each end of the wave guide. When the incoupling condition, eq 1, is fulfilled, the measured intensity shows a sharp peak. N is calculated from the angle α corresponding to the peak maximum.

Table I: Typical Sequence of Optical Measurements[a]

step	solution in cuvette	quantities determined[b]
1	PBS	n_F, d_F
	deposition of bilayer	
2	PBS	n_A, d_A
3[c]	H-PSP or nonspecific Ab	
4	PBS	
5	PSP	
6	PBS	n_B, d_B
7[c]	nonspecific Ab	
8	PBS	
9	α-PSP	
10	PBS	

[a] In each case, 200 μL of a 100 μg/mL solution of protein in PBS was drawn into the cuvette. At the intermediate washing stages, pure PBS was drawn continuously through the cuvette at a rate of 10 μL/s, in order to flush the cuvette after each deposition step. Subscripts A and B refer to the bilayer membrane and the protein layer, respectively. [b] See legend to Figure 1 for the meaning of the symbols. [c] Control experiments (not carried out on every run).

Readings of α corresponding to the transverse electric and transverse magnetic zeroth modes were made every 30 s initially and at longer intervals as deposition decelerated. The sequence of measurements is shown in Table I. All experiments were carried out at 24.0 ± 0.3 °C.

RESULTS

For a uniform[3] layer (of proteins on the bilayer lipid membrane), the surface coverage Γ (mass per unit area) is defined as

$$\Gamma = \Delta\nu d_B \qquad (2)$$

where $\Delta\nu$ is the excess concentration in the layer, defined as

[3] In this context, uniform means that the proteins are statistically uniformly distributed. In fact, the conditions for uniformity are not very stringent, requiring only that the distribution has translational symmetry over distances of order λ.

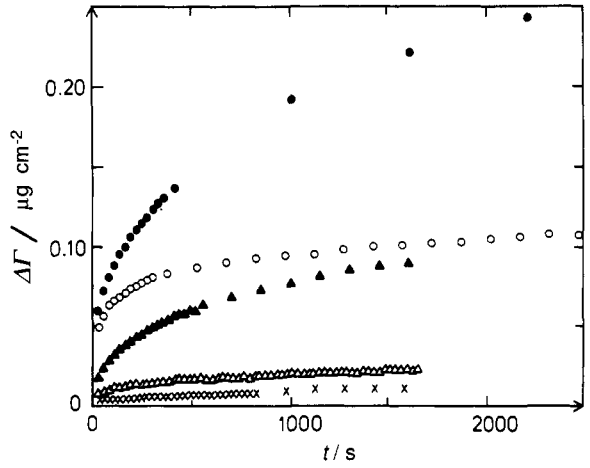

FIGURE 2: Typical data from deposition experiments (early stage). Symbols: ×, nonspecific antibody on $PSP_{membrane}$ (Γ_{PSP} = 0.09 μg/cm^2); Δ, H-PSP on POPC; ▲, nonspecific antibody on POPC; ○, PSP on POPC; ●, α-PSP on $PSP_{membrane}$ (Γ_{PSP} = 0.09 μg/cm^2).

$$\Delta\nu = \nu_B - \nu_b \tag{3}$$

The concentrations ν are given in units of mass per volume; the subscripts B and b refer to the concentration in the layer and in the bulk, respectively. It has been established (de Feijter et al., 1978) that the refractive index n_p of a protein solution is linearly related to the concentration of the protein according to

$$n_p = n_C + \frac{dn}{d\Delta\nu}\Delta\nu \tag{4}$$

where $dn/d\Delta\nu$ has an almost universal value of ~0.182 cm^3/g (de Feijter et al., 1978) and n_C is the refractive index of the buffer solution. Identifying n_p with the refractive index n_B of the protein layer on the lipid membrane and combining eqs 2–4, we obtain

$$\Gamma = \frac{n_B - n_C}{dn/d\Delta\nu} d_B \tag{5}$$

This formula was used to calculate the surface coverage from the measured n_B and d_B data. For each successive step in the reaction sequence, the surface coverage attained in the previous steps was subtracted from the $\Gamma(t)$ values to yield the mass increment $\Delta\Gamma(t)$ for each protein. Figure 2 shows plots of $\Delta\Gamma$ thus calculated versus time. Various controls were also carried out: measurement of the binding of H-PSP to the membrane as a control for lipid-anchored PSP; measurement of the binding of a nonspecific antibody (either the antibodies isolated from the preimmune serum of the same rabbit used to prepare α-PSP or an antibody specific for a randomly chosen protein, in this case a mitochondrial protease) to PSP anchored to the membrane; and measurement of the removal of membrane-bound PSP by bacterial PI-PLC enzyme, to which the PSP lipid moiety is known to be sensitive (Bordier et al., 1986; Schneider et al., 1990).

Qualitatively it can be seen that H-PSP binds to the membrane less and much more slowly than PSP and that the binding of nonspecific antibodies to PSP is almost negligible. In fact, the presence of PSP at the membrane strikingly inhibits the nonspecific binding of antibodies to the membrane itself.

The deposited PSP was treated with bacterial PI-PLC in order to assess the kind of interaction of PSP with the membrane (Figure 3). This enzyme specifically releases alkyl–acyl glycerol from PSP (Schneider et al., 1990). About 35% of the membrane-bound PSP is removed after 3 h of incubation.

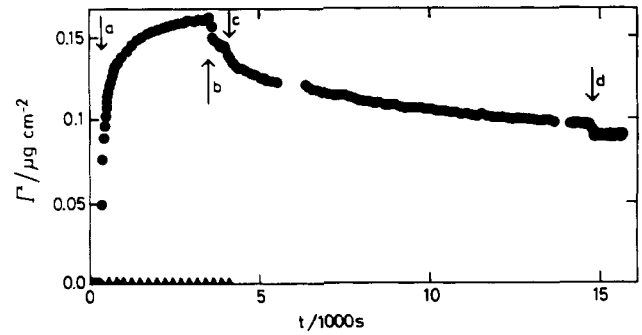

FIGURE 3: Deposition experiment showing removal of PSP from the membrane by the enzyme PI-PLC. (●) Arrows designate the following operations: a, addition of PSP (100 μg/mL) to the cuvette; b, flushing the cuvette with buffer; c, addition of PI-PLC (1 unit/mL); d, flushing with buffer. (▲) PI-PLC (1 unit/mL) added to the bilayer before PSP deposition.

This was not a true end point, however (see Discussion and Figure 8). The concentration of PI-PLC used (1 unit/mL) is enough to quantitatively convert PSP to H-PSP (data not shown).

A rough measure of the degree of reversibility of the binding can be obtained by measuring the loss of mass when the cuvette is flushed with pure buffer.[4] Loss of material from the membrane surface is observed, and a new steady state is rapidly attained. Of course, all binding reactions are formally reversible, but the dissociation rate constant is often so small that in practice it is scarcely measurable by direct observation. The mass removal observed with flushing is essentially a kinetic phenomenon which distinguishes between two populations of bound ligands: those specifically and strongly bound, which do not dissociate over a time scale of tens of minutes or even hours, when the only change in conditions is the removal of the ligand from the bulk solution, and those nonspecifically and weakly bound, which are rapidly and completely dissociated over a time scale of a few minutes. The mass removed is thus a measure of the ratio $\mathcal{M}$ of nonspecific to specific binding. We calculated it using the formula

$$\mathcal{M} = \frac{\Gamma_{\text{before flushing}} - \Gamma_{\text{after flushing}}}{\Delta\Gamma_{\text{before flushing}}} \tag{6}$$

Where deposition of α-PSP on PSP was allowed to continue until a definite plateau was reached, the stoichiometry $\mathcal{S}$ of the binding was determined according to

$$\mathcal{S} = \frac{\Delta\Gamma_{\alpha\text{-PSP}}}{\Delta\Gamma_{PSP}} \frac{M_{PSP}}{M_{\alpha\text{-PSP}}} \tag{7}$$

where M is the molecular weight ($M_{\alpha\text{-PSP}}$ = 140 kDa). In all the other cases, although the rate of binding continuously decreased with time, experiments were not continued long enough for a true plateau to be observed. Such a plateau is only approached asymptotically in diffusion-limited systems (see Discussion). Nevertheless, it was clear that at no stage were multilayers of any of the proteins formed.

Data for $\mathcal{M}$ and $\mathcal{S}$ are collected in Table II.

DISCUSSION

Initial Stage of Kinetics. Where the surface is sparsely occupied (Γ is small), the scheme shown in Figure 4 describes mass transport in the system. We assume that diffusion is the

[4] Flushing the cuvette with buffer in the presence of the membrane alone (Table I, step 2) produced no change in either the thickness or the refractive index of the POPC bilayer.

Table II: Data on the Removal of Mass upon Flushing the Cuvette with Pure Buffer and on the Stoichiometry of Antibody–Antigen Binding

ligand	receptor	$\mathcal{M}^a$ (%)	$\mathcal{S}^b$
H-PSP	POPC bilayer	40 ± 5	
PSP	POPC bilayer	28 ± 2[c]	
nonspecific Ab	POPC bilayer	4 ± 4	
α-PSP	$PSP_{membrane}$	2 ± 2	2.3 ± 0.3[d]
nonspecific Ab	$PSP_{membrane}$	75 ± 25	

[a] Ratio of nonspecific to specific binding, calculated according to eq 6. [b] Stoichiometry of binding, i.e, moles α-PSP/moles PSP at saturation, calculated according to eq 7. [c] For 0.075 ± 0.015 μg/cm² bound PSP. Lower values are found at higher surface coverage (see Discussion and Figure 7). [d] For 0.075 ± 0.015 μg/cm² bound PSP. At this stoichiometry, the protein solution in the cuvette is 3.7% depleted. Lower values are found at higher surface coverage (see Discussion and Figure 7).

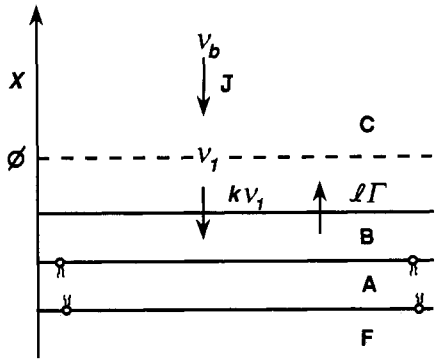

FIGURE 4: Scheme for reversible association at a planar surface with energy barriers, characterized by rate constants k for association and l for dissociation. A quasi steady state is assumed, i.e., $dv_1/dt \approx 0$, and hence the net (diffusion-limited) flux J from the bulk to the thin layer of solution contiguous to the membrane surface plus the flux $l\Gamma$ leaving the surface are equal to the flux kv_1 from the thin contiguous layer to the membrane proper.

only mass transport process taking place in the cuvette; the validity of this assumption (in particular, whether convection can be neglected) is discussed in detail by Ramsden (1992).

The quasi-steady-state condition for this scheme is

$$\frac{dv_1}{dt} = J - kv_1 + l\Gamma \approx 0 \qquad (8)$$

The height of the cuvette is 890 μm, which is almost infinite by a molecular yardstick. J is derived from Fick's laws (Crank, 1975), using the boundary conditions for a semiinfinite medium, and is given by

$$J = (v_b - v_1)\,(D/\pi t)^{1/2} \qquad (9)$$

This equation implies that the bulk protein concentration v_b is constant, a condition which is very nearly true. Taking the nonspecific binding of antibody to the POPC membrane, which gave the most perfect fit to eq 11, as an example, after 1800 s, ca 0.09 μg/cm² have been deposited onto the membrane. For the membrane area of 0.785 cm², this corresponds to a total bound mass of 0.07 μg. Initially, there are 0.07 mL × 100 μg/mL = 7 μg of protein present. Therefore, solution depletion due to adsorption onto the waveguide is only about 1%.

Clearly, from figure 4,

$$\frac{d\Gamma}{dt} = kv_1 - l\Gamma \qquad (10)$$

We use eqs 8 and 9 to eliminate v_1 from eq 10. Its solution is

$$\Gamma = \frac{v_b k}{l}\left[1 - \exp\left[\frac{-2l}{kp}\left[\sqrt{t} - \frac{\ln\,(kp\sqrt{t}+1)}{kp}\right]\right]\right] \qquad (11)$$

where $p = (\pi/D)^{1/2}$. The equilibrium binding, Γ_∞, as $t \to \infty$ equals $v_b k/l$. Since eq 11 cannot be linearized, the data were fit to this equation, using a modified Levenberg–Marquardt nonlinear least-squares method. Significantly, the fits were excellent for nonspecific antibody binding, reasonable over the early stages only for specific antibody binding, and unsatisfactory for PSP binding to the membrane. Where a reasonable set of parameters could be obtained over the early stage, the plot using those same parameters over longer times showed pronounced deviation from the experimental data. These features are illustrated in Figure 5. Numerical results from the fitting are presented in Table III.

Two qualitatively distinct classes of binding appeared, which we call "simple" and "complex" on the basis of whether the data fitted the simple theory embodied in eq 11, together with a third intermediate class. The characteristics of the different classes are summarized in Table IV. It will be noted that goodness of fit does not depend on the fractional surface coverage attained (eqs 8, 10, and 11 are valid for low surface coverage only), because H-PSP deposited on a POPC bilayer only attained 3% of monolayer coverage but nevertheless was at the borderline of the intermediate and complex classes. "Complex" binding appears therefore to be a special property of PSP with or without its lipid anchor.

Late Stage of Kinetics. As deposition of molecules with a strong affinity for a surface proceeds, the surface gradually becomes filled up. For PSP, with its molecular weight of 6.3 × 10⁴ g/mol and an estimated area occupied by one molecule of 23 nm², it is easy to calculate that a complete, densely packed monolayer would correspond to Γ_s = 0.45 μg/cm². If molecules fall on a planar surface and are immediately fixed wherever they happen to land ("random sequential deposition"), the maximum coverage which can be attained is only about 50% of the densely packed value (Feder, 1980; Cooper et al., 1987) because many of the gaps between deposited molecules are too small to accommodate subsequent arrivals. Concomitantly, the rate of binding falls off dramatically with increasing coverage, and the maximum attainable value (i.e., 0.54 of the densely packed value) is approached with kinetics $\sim t^{0.5}$ (if the rate of arrival of molecules from the solution is invariant with time). Since in our diffusion-limited experiments the rate of arrival scales as $t^{0.5}$ (cf. eq 11), this means that kinetics $\sim t^{0.25}$ should be observed as deposition proceeds toward saturation of the surface. Data presented in Figure 6 show that the "simple" binding processes, in which the surface is only sparsely occupied, give kinetics $\sim t^\beta$, with β = 0.5, even for relatively long times, as expected from the absence of effects due to filling up the surface. For the "complex" binding processes, on the other hand, β is not always equal to 0.25, but it is fairly close.

As a corollary of this phenomenon, after as little as 20% of a surface has been covered by a ligand, the surface is effectively blocked against binding by a second high-affinity ligand subsequently presented to it. Provided that the mass of the first ligand deposited is monitored and that it is not necessary to expose the system to the second ligand for a very long time, an intermediate "blocking" step, such as is routinely practiced in affinity assays, should be unnecessary. That this is indeed the case is shown by the very slow rate of binding of nonspecific antibodies to a PSP-covered POPC bilayer, even though nonspecific antibodies have a moderate affinity for the uncovered bilayer (see Figure 1).

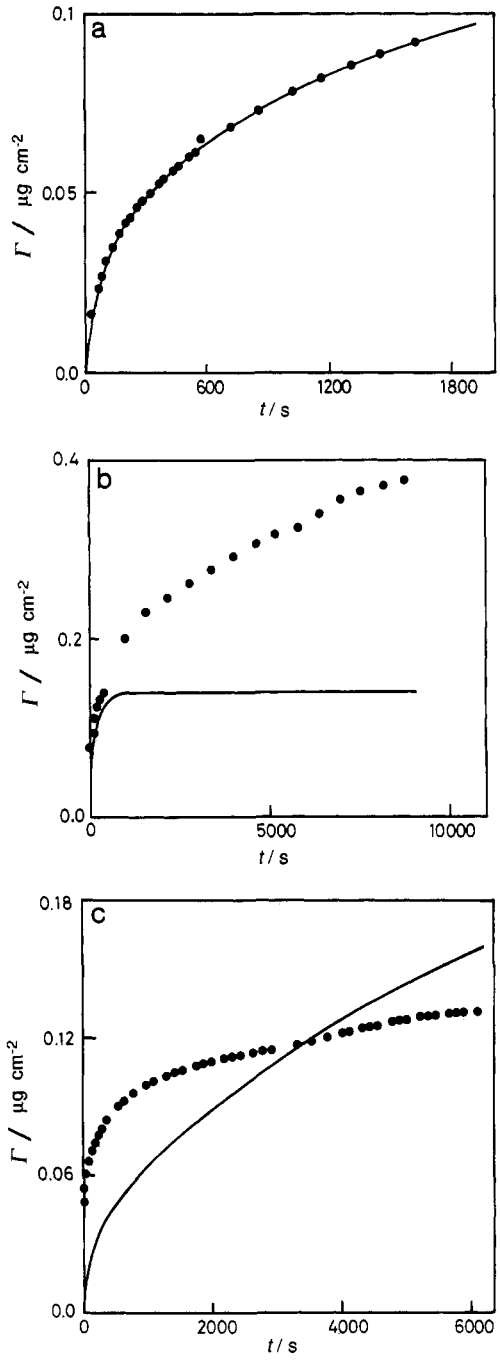

FIGURE 5: Some results from fitting eq 11 to the experimental data. (—) Calculated function; (●) data. (a) Nonspecific antibody binding to the POPC bilayer. (b) α-PSP binding to $PSP_{membrane}$. The plot of eq 11 has been calculated using the parameters (see Table III) determined from the early portion of the curve, for which a reasonable fit is obtainable. (c) PSP binding to the POPC bilayer. The qualitatively different shape of the data compared with eq 11 is plainly apparent.

Two additional features need to be taken into account in our experiments. First, PSP bound or "anchored" to the membrane by its lipid tail will have a certain mobility on the surface, just as an anchored ship will tend to drift and drag its anchor along the sea bed. The PSP molecules should therefore be able to pack together more closely on the surface than in the case of simple random sequential deposition. Whether this closer packing is actually observed depends on the rate of arrival of molecules from the solution relative to the lateral surface mobility of the molecules once they are anchored to the membrane. The highest surface coverage we observed was 0.374 μg/cm², i.e., 83% of a densely packed monolayer. This shows that lateral mobility is indeed high enough to allow a packing denser than that predicted by the simple random sequential deposition model.

Second, when a solution containing α-PSP is presented to a surface on which PSP has been deposited, a fixed and finite number of sites is available to the ligand, and binding should reach a definite plateau. Runs carried out for up to 14 h confirmed this behavior. The mass increment at the plateau was measured and used to calculate the stoichiometry $\mathcal{S}$ using eq 7. Results are shown in Table II. The observed stoichiometry for α-PSP/PSP depends strongly on the density of PSP at the membrane. At 11% surface coverage, it is about 2:1; at 33% coverage, it falls to 1:2; and at 83%, it is only about 1:4. It is expected that the PSP molecule has several epitopes to which the polyclonal antibodies can bind. When the molecules lie at some distance from one another on the surface, more than one of these epitopes will be accessible to the antibodies. The observation of the 2:1 stoichiometry indicates that, at low mean surface coverage, the PSP molecules are not arranged in clusters but are loosely scattered. At higher surface coverage, the antibody/antigen binding ratio decreases from 2:1 to 1:4, indicating a dramatic loss of epitope accessibility. Not only will fewer epitopes be exposed but there may not be enough space for all the remaining exposed epitopes to be bound by the antibodies. Masterson et al. (1988) have shown that there are at least five epitopes accessible on variant surface glycoprotein (VSG) in solution but only one at the surface of an intact VSG coat. Moreover, each antibody is able to bind two antigens, provided that the geometry of the antigen distribution matches that of the antibody binding sites. In addition to the effect of antigen surface coverage on antibody–antigen stoichiometry, at higher antigen surface coverages the kinetics of antibody binding also decreased quite sharply (Figure 7).

Reversibility of PSP Attachment. Figure 7 also presents data showing that the reversibility of PSP binding to the lipid membrane decreases with increasing surface coverage. At low surface coverages ($\Gamma < 0.1$ μg/cm²), 25–30% of membrane-associated PSP can be removed by simply flushing the cuvette with buffer. We can assume that there are two competing binding modes, one via the lipid tail (irreversible) and one via non-tail interactions. H-PSP can only bind via the latter mechanism, and reference to Figure 2 shows that after 1600 s of deposition the mass of H-PSP bound to the membrane is 22% of the mass of PSP bound after the same time. For short washing times only 40% of this non-tail-bound H-PSP is removed, which means that, under the same conditions, we expect 40% × 22% = 9% of PSP to be removed. At high surface coverage this is indeed what we observe, but the fact that 28% is removed at low surface coverage requires an additional mechanism for the removal of PSP. This could be provided by the formation of micelles or aggregates of the lipid-containing PSP at the membrane surface. These micelles would be readily removed from the membrane surface by flushing. In support of this hypothesis, another glycolipid-anchored protein, Thy-1, is known to exist in the form of such micelles, containing about 16 molecules, in the absence of detergent (Tse et al., 1985).

Action of PI-PLC on Membrane-Attached PSP. The removal of deposited PSP by the action of PI-PLC provides further evidence that a fair proportion (at least 40%) of the PSP is bound to the bilayer through its lipid moiety (Figure 3). Plotting the data of Figure 3 after the addition of enzyme to the cuvette as $\ln \Gamma/\Gamma_0$ vs t, where Γ_0 is the surface coverage just before enzyme addition, gave a strongly curved plot. The

Table III: Kinetic Data on Binding[a]

ligand	receptor	k (cm s^{-1})	l (s^{-1})	D (cm^2 s^{-1})	limit of fit: time (s)	limit of fit: Γ^b	limit of fit: c
H-PSP	POPC bilayer	0.06	300	3×10^{-10}	1650	0.024	5%
PSP	POPC bilayer	*d*	*d*	*d*			
nonspecific Ab	POPC bilayer	0.016	11	9.5×10^{-10}	1610	0.09	*e*
α-PSP	$PSP_{membrane}$	0.104	70	1.5×10^{-8}	250[f]	0.11	*e*
nonspecific Ab	$PSP_{membrane}$	0.013	40	10^{-11}	1590	0.012	*e*

[a] Obtained by fitting the early portion of the kinetic runs to eq 11 to the three parameters given in columns 3–5, with $c_0 = 100$ μg/mL. Data up to the limit given in column 6 were included. [b] Surface coverage in units of micrograms per square centimeter, defined by eq 2. [c] Fraction of a complete monolayer. [d] Could not be satisfactorily fitted over any part of the data. [e] Not calculated because the irregular shape of an antibody makes it problematical to determine the area per molecule occupied at the surface. [f] Could not be satisfactorily fitted over longer times. The parameters are not valid for times longer than those shown in the limit column (see Figure 5c).

Table IV: Qualitative Classification of Different Types of Kinetic Behavior Observed during Deposition of Ligand on Receptor and Flushing with Buffer

type	range of fit to eq 11	rate of binding	flush-removable?[a]	example: ligand	example: receptor
simple	entire range	slow	no	nonspecific Ab	POPC bilayer
simple	entire range	slow	all	nonspecific Ab	$PSP_{membrane}$
intermediate	early stages	fast[b]	no	α-PSP	$PSP_{membrane}$
intermediate	very early stages	slow	partly	H-PSP	POPC bilayer
complex	no range	fast	partly[b]	PSP	POPC bilayer

[a] I.e., whether deposited material is rapidly removed when the protein solution in the cuvette is replaced by pure buffer. [b] Depends on the surface coverage of PSP on the membrane.

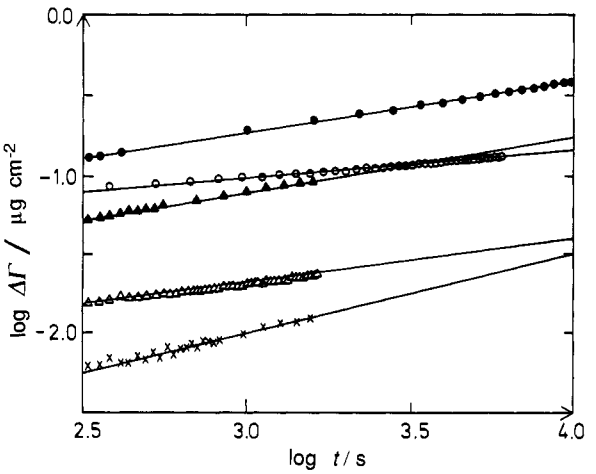

FIGURE 6: Typical data from deposition experiments (late stage) with symbols as in Figure 2. The gradients of the solid lines are as follows: ×, 0.50; △, 0.27; ▲, 0.33; ○, 0.18; ●, 0.35.

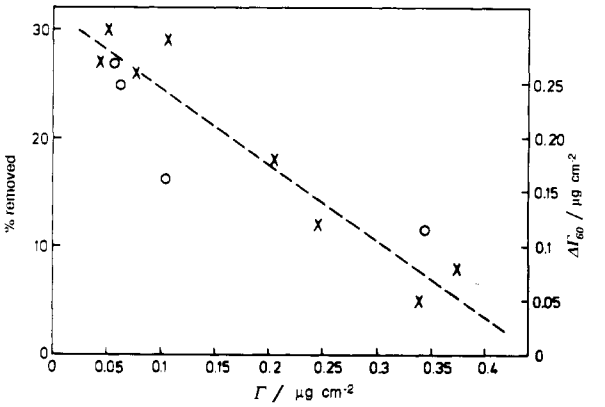

FIGURE 7: Variation of $\mathcal{M}$ (×) for PSP, calculated according to eq 6, and rate of α-PSP binding to PSP, quantified as $\Delta\Gamma_{60}$ = mass increment of α-PSP after 60 min (○), with the mass of PSP bound to the surface, Γ.

removal of membrane-bound PSP is therefore clearly a nonexponential process. A log–log plot of the same data (Figure 8) showed two distinct regions, an early one during which Γ decays as $t^{-0.03}$ and a later one going as $t^{-0.14}$. Although Figure 3 appears to indicate that a plateau is reached after 3 h of incubation with the enzyme, Figure 8 shows that this is not the case.

Some GPI-anchored proteins, such as 5′-nucleotidase, have been shown to be resistant to PI-PLC at the cell surface, although they were sensitive to the same enzyme in detergent solution (Low, 1989). This is also the case with PSP, which cannot be released at all from the parasite by PI-PLC treatment (C. Bordier, personal communication). The fact that PSP can be removed from the artificial bilayer indicates that its resistance to PI-PLC on the parasite surface is not a property of PSP itself but rather of other components of the parasite surface, which may block the action of PI-PLC either by direct interaction with PSP or by preventing the access of macromolecules to the surface. Relevant to this last hypothesis, *Leishmania* expresses two families of abundant glycolipids at its surface, the lipophosphoglycan and the glycoinositol phospholipids, which are present at 5×10^6 and 2×10^7 copies/cell, respectively, and which are likely to form a dense glycocalix at the parasite surface (McConville et al., 1990a,b).

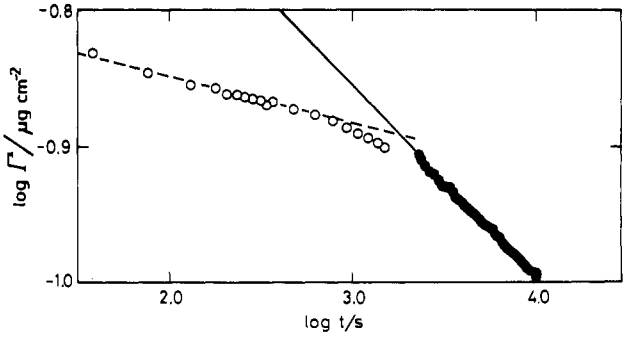

FIGURE 8: Kinetics of enzyme-catalyzed removal of PSP anchored to the membrane. The data are those from Figure 3 (filled circles) between arrows c and d. The two phases are indicated by empty and filled circles, respectively; the straight lines drawn through them have slopes of –0.03 (- - -) and –0.14 (—).

CONCLUSIONS

Deposition of a GPI-anchored protein (PSP) to a supported bilayer lipid membrane can be readily accomplished. Antibodies nonspecific for POPC bind to the membrane with moderate affinity, but as little as 0.2 monolayer of PSP is sufficient to abolish this binding. In practical terms, this means that within about 1 h a packing dense enough to protect the membrane from nonspecific binding of irrelevant antibodies can be achieved, thereby obviating the need for a separate blocking step. As expected, antibodies specific for PSP bind rapidly and irreversibly to PSP, whereas nonspecific antibodies bind very weakly.

PSP lacking its lipid tail has a small affinity for a POPC membrane, but the intact molecule binds faster and less reversibly. Membrane-associated PSP can be at least partially removed by incubation with bacterial PI-PLC, which severs the lipid tail from the rest of the protein. Taken together, these results provide clear evidence that the lipid tail serves to anchor the protein to the membrane.

The novel integrated optics technique used in this investigation allows all stages of the binding process to be followed quantitatively, to high precision, in real time. This precision allows a more detailed and quantitative examination of the binding process than has been possible until now.

Only the weak, nonspecific binding follows a straightforward kinetic model appropriate to binding at a surface. The deviations from simple behavior are most marked for PSP binding to the membrane. Qualitatively, there is evidence for strong interactions between PSP molecules at the surface; e.g., the reversibility of binding decreases with increasing degree of surface coverage.

The rate and ultimate stoichiometry of specific antibodies binding to PSP anchored at the membrane fall sharply as the surface density of antigen (PSP) increases. At low surface coverage the stoichiometry of antibody/antigen is 2:1; at intermediate coverage it falls to 1:2, and at the densest coverages it is only 1:4, indicating progressive loss of epitope accessibility.

ACKNOWLEDGMENT

We thank C. Bordier and M. A. J. Ferguson for valuable discussions.

REFERENCES

Bordier, C., Etges, R. J., Ward, J., Turner, M. J., & Cardoso de Almeida, M. L. (1986) *Proc. Natl. Acad. Sci. U.S.A. 83*, 5988–5991.

Bouvier, J., Etges, R. J., & Bordier, C. (1985) *J. Biol. Chem. 260*, 15504–15509.

Bouvier, J., Bordier, C., Vogel, H., Reichelt, R., & Etges, R. J. (1989) *Mol. Biochem. Parasitol. 37*, 235–246.

Crank, J. (1975) *The Mathematics of Diffusion*, 2nd ed., Clarendon Press, Oxford, England.

de Feijter, J. A., Benjamins, J., & Veer, F. A. (1978) *Biopolymers 17*, 1759–1772.

Hoh, J. H., & Hansma, P. K. (1992) *Trends Cell Biol. 2*, 208–213.

Hönig, D., & Möbius, D. (1991) *J. Phys. Chem. 95*, 4590–4592.

Langmuir, I., & Schaefer, V. J. (1937) *J. Am. Chem. Soc. 60*, 1351–1360.

Low, M. G. (1989) *Biochim. Biophys. Acta 988*, 427–454.

Masterson, W. J., Taylor, D., & Turner, M. J. (1988) *J. Immunol. 140*, 3194–3199.

McConville, M. J., Thomas–Oates, J. E., Ferguson, M. A. J., & Homans, S. W. (1990a) *J. Biol. Chem. 265*, 19611–19623.

McConville, M. J., Homans, S. W., Thomas-Oates, J. E., Dell, A., & Bacic, A. (1990b) *J. Biol. Chem. 265*, 7385–7394.

Ramsden, J. J. (1992) *J. Phys. Chem. 96*, 3388–3391.

Schmitt, F.-J., Meller, P., Ringsdorf, H., & Knoll, W. (1990) *Prog. Colloid Polym. Sci. 83*, 136–145.

Schneider, P., Ferguson, M. A. J., McConville, M. J., Mehlert, A., Homans, S. W., & Bordier, C. (1990) *J. Biol. Chem. 265*, 16955–16964.

Spikhalskii, A. A. (1986) *Opt. Quantum Electron. 18*, 103–114.

Takoshima, T., Masuda, A., & Mukasa, K. (1992) *Thin Solid Films 210/211*, 51–56.

Tiefenthaler, K., & Lukosz, W. (1989) *J. Opt. Soc. Am. B. 6*, 209–220.

Tien, P. K. (1971) *Appl. Opt. 10*, 2395–2413.

Tse, A. G. D., Barclay, A. N., Watts, A., & Williams, A. F. (1985) *Science 230*, 1003–1008.